

Topoisomerase II α -dependent and -independent apoptotic effects of dexrazoxane and doxorubicin

Tiandong Yan,¹ Shiwei Deng,¹ Annegret Metzger,¹ Ute Gödtel-Armbrust,¹ Andrew C.G. Porter,² and Leszek Wojnowski¹

¹Department of Pharmacology, Johannes Gutenberg University, Mainz, Germany and ²Department of Haematology, Faculty of Medicine, Imperial College London, London, United Kingdom

Abstract

Coadministration of the iron chelator dexrazoxane reduces by 80% the incidence of heart failure in cancer patients treated with anthracyclines. The clinical application of dexrazoxane is limited, however, because its ability to inhibit topoisomerase II α (TOP2A) is feared to adversely affect anthracycline chemotherapy, which involves TOP2A-mediated generation of DNA double-strand breaks (DSB). Here, we investigated the apoptotic effects of dexrazoxane and the anthracycline doxorubicin, alone and in combination, in a tumor cell line with conditionally regulated expression of TOP2A. Each drug caused apoptosis that was only partly dependent on TOP2A. Unexpectedly, dexrazoxane was found to cause TOP2A depletion, thereby reducing the doxorubicin-induced accumulation of DSB. Despite this latter effect, dexrazoxane showed no adverse effect on doxorubicin-induced apoptosis. This could be explained by the TOP2A-independent apoptotic effects of each drug: those of doxorubicin included TOP2A-independent DSB formation and depletion of intracellular glutathione, whereas those of dexrazoxane were caspase independent. In conclusion, both doxorubicin and dexrazoxane induce apoptosis via TOP2A-dependent and TOP2A-independent mechanisms, the latter compensating for the reduction in cell killing due to dexrazoxane-induced TOP2A depletion. These observations suggest an explanation for the absence of adverse dexrazoxane effects on clinical responses to doxorubicin. [Mol Cancer Ther 2009;8(5):1075–85]

Received 11/14/08; revised 2/16/09; accepted 3/9/09; published OnlineFirst 5/5/09.

Grant support: NGFN2 grant O1GS0421 of the German Federal Ministry for Education and Science (L. Wojnowski).

The costs of publication of this article were defrayed in part by the payment of page charges. This article must therefore be hereby marked *advertisement* in accordance with 18 U.S.C. Section 1734 solely to indicate this fact.

Note: T. Yan and S. Deng contributed equally to this work.

Requests for reprints: Leszek Wojnowski, Department of Pharmacology, Johannes Gutenberg University, Obere Zahlbacher Str. 67, D-55101 Mainz, Germany. Phone: 49-6131-39-33460/37170; Fax: 49-6131-39-36611. E-mail: wojnowski@uni-mainz.de

Copyright © 2009 American Association for Cancer Research.

doi:10.1158/1535-7163.MCT-09-0139

Introduction

Anthracyclines belong to the most successful drugs used in oncology because they are effective against a wide range of common cancers (1). The most important limitation of their application is the congestive heart failure, which develops in 5% to 20% of patients years to decades after the chemotherapy (2). The bisdioxopiperazine dexrazoxane (ICRF-187) reduces the risk of anthracycline-induced congestive heart failure by ~80% (3). The cardioprotective effect has been attributed to iron trapping by ADR-925, an EDTA-like product of dexrazoxane hydrolysis. Iron trapping prevents the formation of cardiomyocyte-damaging hydroxyl radicals triggered by “redox cycling” of anthracyclines (4).

Considering the impressive cardioprotective effect of dexrazoxane, its coadministration with anthracyclines to cancer patients has been disappointingly limited. This is mostly due to the persisting fears that combining these drugs may adversely affect outcomes of cancer treatments. Although these fears have been refuted in several randomized clinical studies (3, 5), it is likely that dexrazoxane does indeed interact with anthracyclines in cancer cells. Dexrazoxane (not its cardioprotective derivative ADR-925) binds and inhibits topoisomerase II α (TOP2A), a major target of anthracyclines. Dexrazoxane locks TOP2A dimers in a “closed clamp” configuration, which differs from the irreversible “poisoning” of the enzyme by anthracyclines (4). The combined effects of dexrazoxane and anthracyclines have been previously tested in several cell and animal cancer models. The results variously indicated synergy, addition, and antagonism between these drugs in their ability to induce cell killing (6, 7). The outcome varied with the cell type, dexrazoxane concentration, addition sequence, and exposure times (6, 8). No satisfactory explanation has been found for these disparate observations.

We are convinced that a better acceptance of dexrazoxane as a cardioprotectant in anthracycline therapies can be achieved only through a more complete understanding of cancer cell-killing effects of these drugs. This issue is of paramount clinical importance, because the application of anthracyclines in oncology shows no signs of abating and dexrazoxane remains the only clinically proven remedy against congestive heart failure associated with their use (3). We therefore investigated, alone and in combination, the mechanisms of cancer cell killing by dexrazoxane and by doxorubicin, the most widely used anthracycline. For several reasons, we focused on the importance of TOP2A. Firstly, both drugs share TOP2A as a major target and the individually variable expression level of TOP2A in breast tumors is being developed as a marker predictive for anthracycline response (9). Further, anthracyclines probably kill cancer cells by several mechanisms independent from TOP2A “poisoning.” In addition to the inhibition of

enzymes such as helicases, they may exert direct DNA-related effects including binding, alkylation, crosslinking, and strand separation (10). Additional DNA and cell membrane damage could be brought about by "redox cycling" of anthracyclines (10). However, the individual contributions of these processes to the antitumor effects of anthracyclines are unknown. Even less understood is the cell-killing effect of dexrazoxane, which occurs in the absence of extensive DNA damage (11, 12). Especially puzzling is the contrast between the cytotoxic effect of dexrazoxane on cancer cells and its protective effect on anthracycline-exposed cardiomyocytes.

To differentiate between TOP2A-dependent and TOP2A-independent effects of dexrazoxane and doxorubicin, we used HTETOP cells, a human tumor cell line that expresses TOP2A exclusively from a tetracycline-regulated transgene (13). This conditionality of TOP2A expression avoids the cellular lethality that would result from a constitutive TOP2A knockout (14). Thus, in the first 2 days following tetracycline addition, HTETOP cells lose up to ~95% of their TOP2A but continue to proliferate without any major changes in morphology or ploidy (13) or, as we show below, in the expression of genes other than TOP2A. Using this unique tool, we were able, for the first time, to clearly differentiate between TOP2A-dependent and TOP2A-independent effects of doxorubicin and dexrazoxane. Based on these results, we suggest an explanation for the somewhat counterintuitive fact that dexrazoxane does not adversely affect doxorubicin-based cancer treatments.

Materials and Methods

Cell Culture

HTETOP cells, derived from the human fibrosarcoma cell line HT1080, were described previously (13). The expression level of TOP2A in HTETOP cells can be reversibly depressed by the addition of tetracycline such as doxycycline. HTETOP cells were cultured in a DMEM supplemented with 10% heat-inactivated fetal bovine serum, 40 units/mL penicillin, 40 μ g/mL streptomycin, 20 mmol/L HEPES, 10 mmol/L MEM sodium pyruvate, and 4% (v/v) nonessential amino acids (all from PAA Laboratories). Cells were maintained in a CO₂ (5%) incubator at 37°C. Dexrazoxane hydrochloride was from Chiron and doxorubicin was from Pfizer.

Cytotoxicity Assay

IC₅₀ values for doxorubicin and dexrazoxane in HTETOP cells were determined using 3-(4,5-dimethylthiazol-2-yl)-2,5-diphenyltetrazolium bromide assays. Cells were seeded in triplicate at 7,000 per well in a 96-well plate and treated with variable concentrations of doxorubicin or dexrazoxane for 24 h. 3-(4,5-Dimethylthiazol-2-yl)-2,5-diphenyltetrazolium bromide assay buffer (20 μ L; 5 mg/mL) was added to each well followed by 4 h incubation at 37°C. After a wash with PBS, cells were incubated with DMSO for 10 min and the absorbance was measured at 570 nm. IC₅₀ was calculated by nonlinear regression analysis using GraphPad Prism version 5.01.

Fluorescence-Activated Cell Sorting Analysis

Fluorescence-activated cell sorting (FACS) assays were done to detect apoptosis in cells stained with Annexin V-FITC (BD Pharmingen) and To-Pro-3 iodide (Invitrogen). Subconfluent cells were gently harvested using accutase. Cell pellet was obtained by low-speed centrifugation (400 \times g, 5 min, 4°C). After two washes with PBS, the cell pellet was resuspended in 400 μ L of 1 \times binding buffer. Cell suspension (100 μ L) was transferred to a new 5 mL tube in the presence of 2 μ L Annexin V-FITC buffer and incubated for 10 min in darkness at room temperature. Finally, 1 μ L To-Pro-3 solution was added to the mixture and further incubated for 5 min in darkness followed by the addition of 400 μ L of 1 \times binding buffer. Flow cytometry analysis was done within 1 h.

Reduced Glutathione and Oxidized Glutathione Detection

Reduced glutathione (GSH) and oxidized glutathione (GSSG) contents were measured as described previously (15). Briefly, cells were lysed at 4°C for 20 min in a lysis buffer containing 200 mmol/L NaCl, 100 mmol/L Tris-HCl, 1% Triton X-100, and a protease inhibitor cocktail. After centrifugation at 4,000 \times g for 5 min, the supernatant was used for protein concentration and total GSH measurement. The supernatant was mixed with 0.73 mmol/L 5,5-dithiobis(2-nitrobenzoic acid) and 0.24 mmol/L NADPH in a reaction buffer containing 143 mmol/L NaH₂PO₄ and 6.3 mmol/L EDTA (pH 7.5). Absorbance at 415 nm was immediately recorded after the addition of 1.2 units/mL glutathione reductase. The total amount of GSH was calculated according to the GSH standard curve. GSSG was measured using the same method after trapping of GSH by 2-vinylpyridine. GSH was quantified by subtracting GSSG amount from the total GSH amount.

Caspase-3/7 Activity Measurement

Caspase-3/7 activity was measured with the Caspase-Glo 3/7 Assay Kit (Promega) according to the manufacturer's instructions on cells seeded in a 96-well plate. At the end of the specified drug treatments, cells were incubated with the Caspase-Glo 3/7 reagent at room temperature for 30 min. Luminescence of each well was recorded in a plate-reading luminometer. The luminescence intensity was expressed as relative light units.

Western Blot

Cells were lysed in a radioimmunoprecipitation assay buffer containing 50 mmol/L Tris-HCl (pH 7.4), 150 mmol/L NaCl, 1% Igepal CA-630, 0.5% sodium deoxycholate, 0.1% SDS, and a protease inhibitor cocktail. For TOP2A detection, 50 μ g/mL DNase I and 5 mmol/L MgCl₂ (final concentrations) were added to the lysates to release TOP2A protein from the DNA-TOP2A complexes. Protein concentrations were determined by Bradford assay (Bio-Rad Protein Dye Reagent). Protein (20 μ g) was separated by SDS-polyacrylamide gels (7.5% for detection of TOP2A and TOP2B and 12% for γ -H2AX and caspase-8) and transferred onto polyvinylidene fluoride membranes. After blocking in TBS-T buffer [10 mmol/L Tris-HCl (pH 7.4), 150 mmol/L NaCl, 0.05% Tween 20] containing 5% nonfat milk for 1 h at

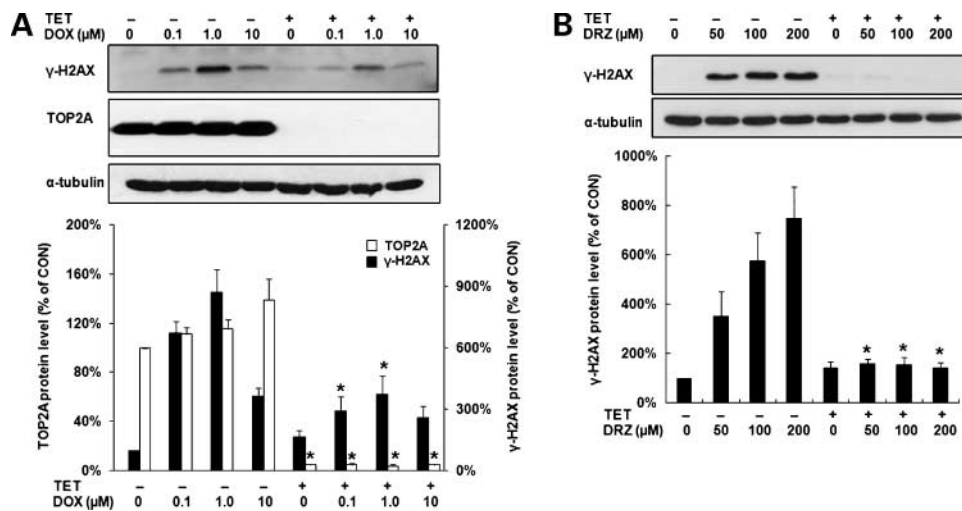


Figure 1. DSB formation, assessed as γ -H2AX foci, and TOP2A level in HTETOP cells in response to doxorubicin and dexrazoxane. **A**, γ -H2AX and TOP2A protein levels determined by Western blot in untreated or tetracycline pretreated (1 μ g/mL, 24 h) cells followed by 24 h incubation at the specified doxorubicin concentrations. Unless otherwise specified, Western blots were repeated at least three times and results were quantified, normalized to the loading controls, and expressed as percentage of untreated cells (CON; cells without any treatment). *, $P < 0.05$, compared with cells treated with the same doxorubicin concentration but without tetracycline. **B**, γ -H2AX formation assessed by Western blot in response to the indicated dexrazoxane concentrations applied over 24 h. *, $P < 0.05$, compared with cells treated with the same dexrazoxane concentration but without tetracycline.

room temperature, the membranes were incubated with mouse monoclonal antibody against human TOP2A (1:2,000; Stressgen), TOP2B (1:1,000; BD Pharmingen), γ -H2AX (1:2,000; Abcam), caspase-8 (1:2,000; BD Pharmingen), α -tubulin (1:20,000; Dianova), or GAPDH (1:5,000; Santa Cruz Biotechnology) at 4°C overnight. After washing in TBS-T three times, membranes were incubated with anti-mouse IgG (1:20,000; Sigma) for 1 h at room temperature. Bands were visualized by the ECL+ detection method (Amersham Pharmacia Biotech). Densitometric analysis of the protein bands was done using the NIH Image J freeware.

RNA Microarray Analysis

Expression changes induced by tetracycline or dexrazoxane were evaluated by high-density oligonucleotide RNA microarrays as described previously (16). Briefly, RNA was extracted from triplicates of untreated or tetracycline-treated cells and cDNA was synthesized by reverse transcription for *in vitro* cRNA synthesis. After biotin labeling, purification, and fragmentation, cRNA was hybridized to Human Genome U133 Plus 2.0 GeneChips (Affymetrix). The raw data obtained from scanned chips were analyzed by robust multiarray analysis (17) for background adjustment and normalization. The microarray data are available at the Gene Expression Omnibus at [http://www.ncbi.nlm.nih.gov/geo/\(GSE14886\)](http://www.ncbi.nlm.nih.gov/geo/(GSE14886)).

TaqMan Assay

Total RNA was isolated from the cells with the peqGOLD Total RNA Kit according to the manufacturer's instructions. Total RNA (1 μ g) was reverse transcribed using the High-Capacity cDNA Reverse Transcription Kit (Applied Biosystems) in a total volume of 20 μ L. cDNA (1 μ L) was mixed with a TaqMan Universal PCR Master Mix (Applied Biosystems) and TOP2A Gene Expression Assay (Hs00172214_m1; Applied Biosystems) according to the manufacturer's re-

commendations and real-time PCR was conducted in a 7900HT iCycler from Bio-Rad Laboratories. 18S rRNA (Hs99999901_s1; Applied Biosystems) was used for normalization. The results were calculated using the $\Delta\Delta$ Ct method.

Statistical Analysis

All experiments were conducted at least three times. Results are expressed as mean \pm SE. Between groups, comparisons were made with Student's *t* test or ANOVA; statistical significance was defined by $P < 0.05$.

Results

We wanted to characterize the contribution of TOP2A to apoptosis induced by doxorubicin and dexrazoxane. To this end, HTETOP cells were incubated for 24 h with 1 μ g/mL of the tetracycline doxycycline. In agreement with the original publication (13), tetracycline depleted the TOP2A (e.g., Fig. 1A) but not TOP2B (data not shown) protein. This was due to the \sim 100-fold reduction in the expression of mRNA derived from the tetracycline-dependent TOP2A transgene as confirmed by TaqMan (data not shown) and by expression profiling of the entire transcriptome using RNA microarrays (Fig. 2A). The latter experiment showed an extraordinarily specific effect on TOP2A expression: the only mRNAs with significantly changed levels following addition of tetracycline for 24 h were TOP2A transcripts.

TOP2A-depleted (tetracycline-treated) and control (tetracycline-untreated) cells were then exposed to doxorubicin and dexrazoxane at concentrations corresponding to the range measured in blood of patients treated with either drug. In addition, we tested a supraclinical doxorubicin concentration of 10 μ mol/L. For comparison, the IC₅₀ values of the cytotoxicity/viability 3-(4,5-dimethylthiazol-2-yl)-2,5-diphenyltetrazolium bromide assay for doxorubicin

and dexrazoxane in HTETOP cells were 0.52 $\mu\text{mol/L}$ and 7.45 mmol/L , respectively. Doxorubicin induced apoptosis in an exposure time-dependent manner (Fig. 2B) and concentration-dependent manner (Fig. 2C) in both untreated and tetracycline-pretreated HTETOP cells. However, the apoptosis in tetracycline-pretreated (TOP2A-depleted) cells was abolished at 0.1 $\mu\text{mol/L}$ doxorubicin and reduced by $\sim 50\%$ at 1 and 10 $\mu\text{mol/L}$ doxorubicin (Fig. 2C). Dexrazoxane also induced apoptosis in a concentration-dependent manner (Fig. 2D) and exposure time-dependent manner (Fig. 3B, *bottommost*). Depletion of TOP2A by tetracycline reduced by $\sim 50\%$ the fold increase in apoptosis induced by ≥ 25 $\mu\text{mol/L}$ dexrazoxane (Fig. 2D).

These results showed both TOP2A-dependent and TOP2A-independent apoptosis induced by either drug. To better delineate the apoptotic pathways involved, we determined the expression or activity of several cellular parameters previously implicated in the cytotoxic effects of doxorubicin and dexrazoxane, beginning with double-strand breaks (DSB), TOP2A expression, and oxidative stress parameters. DSB arise through TOP2A "poisoning" by doxorubicin and are detectable as $\gamma\text{-H2AX}$ foci (18) fol-

lowing the proteasome-mediated degradation of doxorubicin-TOP2A-DNA complexes (10). As shown in Fig. 1A, clinically relevant doxorubicin concentrations of 0.1 and 1 $\mu\text{mol/L}$ (19) indeed increased DSB levels. In agreement with previous observations (20), the DSB increase at the supraclinical doxorubicin concentration of 10 $\mu\text{mol/L}$ was much smaller. Although incompletely understood, this latter effect may reflect doxorubicin toxicity toward the proteasome, which is necessary for $\gamma\text{-H2AX}$ foci detection (21). In the absence of tetracycline, doxorubicin also resulted in a statistically nonsignificant trend toward a moderate (< 2 -fold) accumulation of the TOP2A protein (Figs. 1A and 3A), most likely reflecting the diminished degradation of the doxorubicin-"poisoned" enzyme. TOP2A depletion reduced the DSB formation by 0.1 and 1.0 $\mu\text{mol/L}$ doxorubicin (Fig. 1A). This result indicated that, although doxorubicin induces DSB via TOP2A "poisoning," DSB may also arise via mechanisms independent from TOP2A. DSB formation was also detected following dexrazoxane treatment (Fig. 1B). In contrast to doxorubicin, dexrazoxane-induced DSB formation was entirely dependent on TOP2A as shown by the absence of DSB in TOP2A-depleted cells.

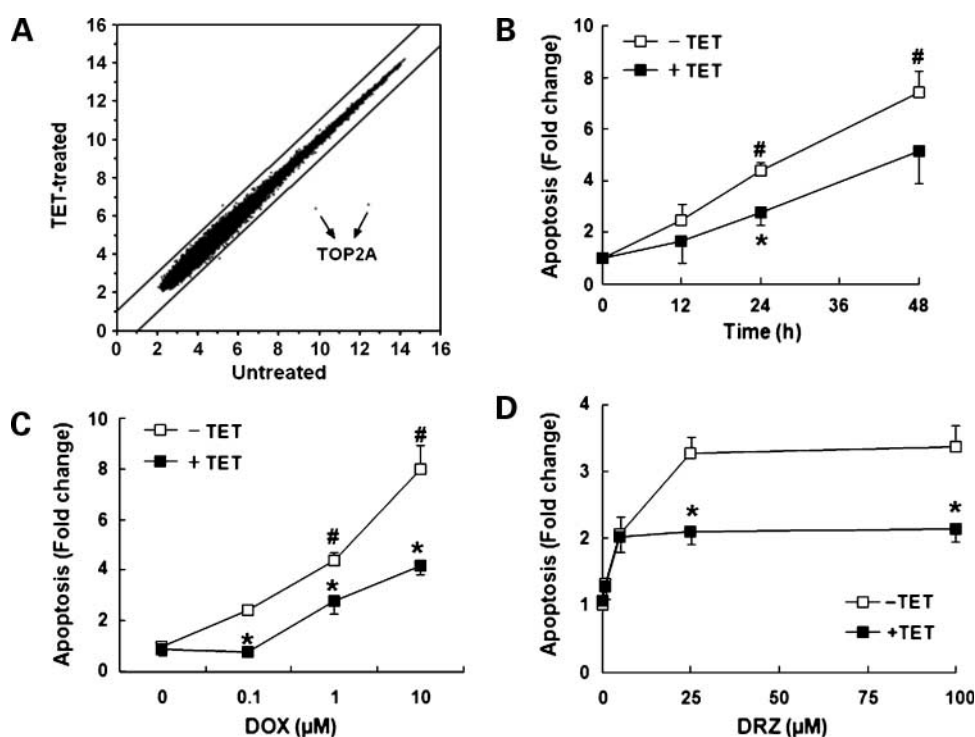


Figure 2. Involvement of TOP2A in doxorubicin- and dexrazoxane-induced apoptosis in HTETOP cells. **A**, scatter plot of the comparison between genome-wide gene expression profiles, expressed as \log_2 , of untreated and tetracycline-treated (1 $\mu\text{g/mL}$ tetracycline for 24 h) HTETOP cells. Genes with < 2 -fold expression differences are contained between the two diagonal lines. Arrows, two probe sets targeting TOP2A. **B**, time course and TOP2A dependency of apoptosis induced by doxorubicin as assessed by Annexin V-FITC staining and FACS analysis. Untreated or TOP2A-depleted (1 $\mu\text{g/mL}$ tetracycline for 24 h) cells were incubated with 1 $\mu\text{mol/L}$ doxorubicin for the indicated periods. Results are expressed as fold change increase in apoptosis in comparison with cells without doxorubicin treatment at 0 h. #, $P < 0.05$, compared with untreated cells at 0 h; *, $P < 0.05$, compared with tetracycline-untreated cells at the same time point. **C**, effect of tetracycline pretreatment (1 $\mu\text{g/mL}$, 24 h) on apoptosis induced by 24 h of subsequent incubation with the indicated doxorubicin concentrations. #, $P < 0.05$, compared with untreated cells (0 $\mu\text{mol/L}$); *, $P < 0.01$, compared with cells treated with the same doxorubicin concentration but without tetracycline. **D**, dexrazoxane-induced apoptosis detected by Annexin V-FITC staining and FACS analysis in cells incubated for 24 h at the indicated concentrations of dexrazoxane with or without tetracycline pretreatment (1 $\mu\text{g/mL}$, 24 h). *, $P < 0.05$, compared with cells treated with the same dexrazoxane concentration but without tetracycline.

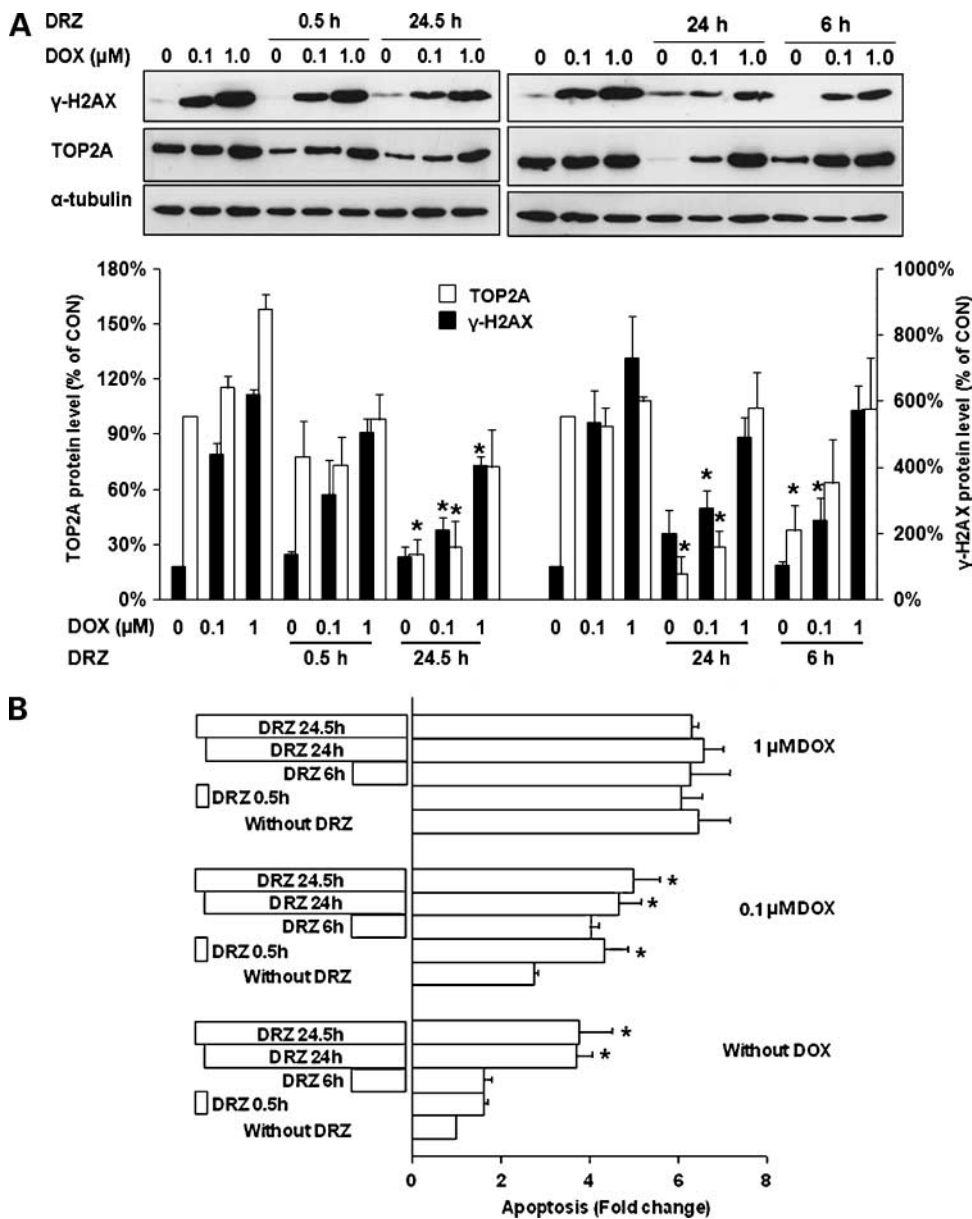


Figure 3. Effect of coapplication of dexrazoxane and doxorubicin on DSB formation, TOP2A protein level, and apoptosis. **A**, DSB, assessed as γ-H2AX foci, and TOP2A protein level following 0.1 or 1 μmol/L doxorubicin and/or 100 μmol/L dexrazoxane administered for the indicated periods schematically depicted in **B**, that is for 0.5 h before doxorubicin (0.5 h), for 0.5 h before and subsequently together with doxorubicin (24.5 h), together with doxorubicin (24 h), and during the last 6 h of the incubation with doxorubicin (6 h). *, *P* < 0.05, compared with cells treated with the same doxorubicin concentration but without dexrazoxane. **B**, apoptosis detected by Annexin V-FITC staining and FACS analysis in cells treated under the same conditions as in **A**. *, *P* < 0.05, compared with cells treated with the same concentration of doxorubicin but without dexrazoxane.

Unexpectedly, we found that dexrazoxane decreased, in a concentration-dependent manner, the intracellular TOP2A protein content of HTETOP cells (Fig. 4A, top; see Supplementary Figure³ for the quantitative results of all Western blots from Fig. 4). This effect is unlikely to reflect the well-known phenomenon of “band depletion,” which is caused

by the rapid formation of dexrazoxane-DNA-TOP2A complexes that remain in sample wells during electrophoresis (22), because all samples were treated with DNase I to release TOP2A from the complexes with DNA before analysis. Furthermore, TOP2A protein decreased slowly, over a period of 24 h (Fig. 4A, bottom; Supplementary Fig. B),³ whereas “band depletion” is detectable within minutes after the incubation onset (22). Because dexrazoxane has been recently shown to trigger a proteasome-mediated degradation of TOP2B (20),

³ Supplementary material for this article is available at Molecular Cancer Therapeutics Online (<http://mct.aacrjournals.org/>).

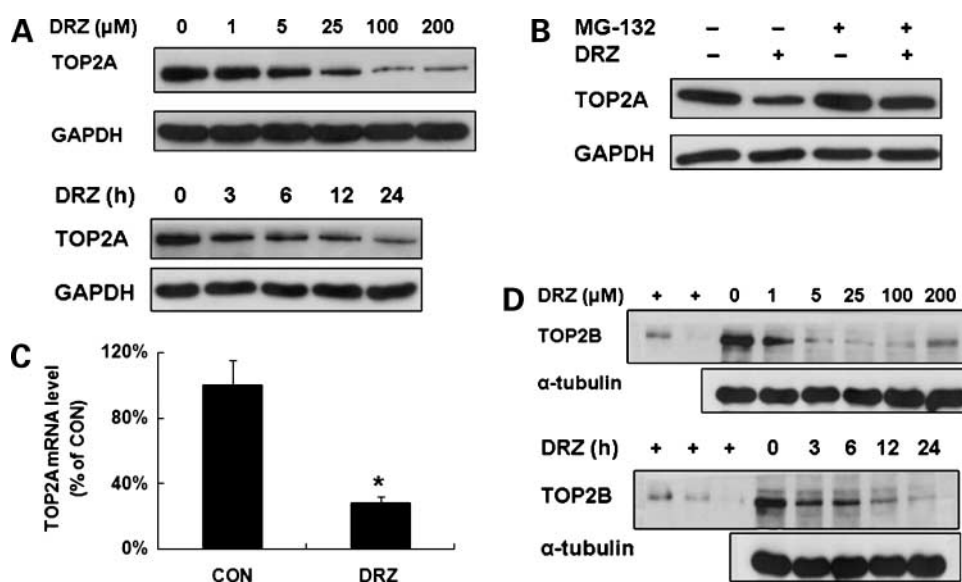


Figure 4. TOP2A and TOP2B depletion by dexrazoxane in HTETOP cells. **A**, TOP2A protein level detected by Western blot in cells exposed to the specified concentrations dexrazoxane for 24 h (*top*) or cells treated with 100 $\mu\text{mol/L}$ dexrazoxane for the specified periods (*bottom*). **B**, effect of the proteasome inhibitor MG-132 (0.25 $\mu\text{mol/L}$, 24 h) on the dexrazoxane-induced (100 $\mu\text{mol/L}$, 24 h) TOP2A depletion as assessed by Western blot. **C**, effect of dexrazoxane (100 $\mu\text{mol/L}$, 24 h) on the TOP2A transcript level assessed by TaqMan assay. *, $P < 0.01$, compared with untreated cells. **D**, TOP2B protein level detected by Western blot in cells exposed to the specified concentrations dexrazoxane for 24 h (*top*) or cells treated with 100 $\mu\text{mol/L}$ dexrazoxane for the specified periods (*bottom*). Purified recombinant human TOP2B protein was used as a positive control (+): *top*, 40 and 20 ng in lanes 1 and 2, respectively; *bottom*, 40, 30, and 20 ng in lanes 1 to 3, respectively. The quantitative results from these Western blots are shown in Supplementary Figure.³

we investigated the importance of proteasome in the dexrazoxane-induced TOP2A depletion. Dexrazoxane-induced TOP2A depletion could not be prevented by the proteasome inhibitor MG-132 (0.25 $\mu\text{mol/L}$; Fig. 4B). In most experiments, MG-132 also increased TOP2A level in dexrazoxane-untreated cells (Fig. 4B), casting doubts on the specificity of its antagonistic effect on dexrazoxane. In search of an alternative explanation for TOP2A depletion, we measured mRNA expression level of TOP2A following dexrazoxane (100 $\mu\text{mol/L}$, 24 h) exposure. Dexrazoxane clearly reduced TOP2A mRNA (Fig. 4C). This effect was also observed in the parental, nontransgenic cell line HT1080 (data not shown). In contrast to HTETOP cells, TOP2A expression in HT1080 cells is driven by a normal, endogenous TOP2A promoter. The results from both cell lines taken together suggest that dexrazoxane decreases TOP2A mRNA level via a promoter-independent mechanism. Regardless of its precise mechanism, the reduction of TOP2A mRNA was remarkably specific as shown by genome-wide RNA microarray analysis of HTETOP cells exposed to 100 $\mu\text{mol/L}$ dexrazoxane for 24 h. In this analysis, TOP2A was one of only two genes with expression level altered by dexrazoxane (3-fold decrease), the other being the activating transcription factor 3 (2.5-fold increase). In agreement with a recent report (20), dexrazoxane also caused TOP2B depletion in a concentration- and time-dependent manner (Fig. 4D). This effect was observed in the absence of any changes of TOP2B transcript level as assessed by genome-wide RNA microarrays. Taken together, these results indicate that the dexrazoxane-induced depletion of TOP2A and TOP2B occur via different mechanisms.

Further differences in the cellular responses to doxorubicin and dexrazoxane were revealed by measurements of glutathione content following drug exposure. Glutathione [specifically the ratio between its oxidized (GSSG) and its reduced (GSH) forms] is an indicator of oxidative stress, which has been inconclusively implicated in doxorubicin response (10). The proportion of total glutathione (GSSG + GSH) that was GSSG remained unchanged (8-11%) following exposure to doxorubicin (Fig. 5A). On the other hand, up to 60% of the total glutathione content in HTETOP cells was depleted, in a concentration-dependent manner, following treatment with doxorubicin. As a positive control, an inhibitor of glutathione synthesis (buthionine sulfoximine; ref. 23) was found to deplete total glutathione by >95% (Fig. 5A). The compensation of glutathione loss by coinubation with the cell membrane-permeable glutathione ethyl ester reduced the apoptosis rate by 46% (Fig. 5B). This indicated that the depletion of total glutathione contributed to apoptosis by doxorubicin. Strikingly, glutathione ethyl ester had no effect on DSB formation by 1 $\mu\text{mol/L}$ doxorubicin, although it prevented DSB evoked by H_2O_2 (Fig. 5C). This suggested that the portion of doxorubicin-induced apoptosis associated with loss of total glutathione is not mediated by DSB. In contrast to doxorubicin, dexrazoxane (100 $\mu\text{mol/L}$) affected neither the total glutathione nor the ratio between its oxidized and reduced forms (data not shown). Accordingly, supplementation with glutathione ethyl ester had no effect on dexrazoxane-induced apoptosis (data not shown).

Responses to doxorubicin and dexrazoxane showed more similarities with respect to the involvement of p53 and

caspses. Although these factors play central roles in apoptosis triggered by DNA damage, the importance of p53 to the doxorubicin response is controversial (24, 25) and to the dexrazoxane response unknown. Apoptosis induced in HTE-TOP cells by 0.1 and 1 $\mu\text{mol/L}$ doxorubicin or by 100 $\mu\text{mol/L}$ dexrazoxane was totally abolished by the recently developed p53 inhibitor PFT- μ (Fig. 6A and B). PFT- μ inhibits p53 binding to mitochondria via reducing its affinity to anti-apoptotic proteins Bcl-xL and Bcl-2 without affecting the p53-dependent transactivation (26). In contrast, the inhibitor of the p53 transcriptional pathway PFT- α (27) had no effect on apoptosis (Fig. 6A and B). Furthermore, doxorubicin and dexrazoxane each activated caspase-3/7, and activation was attenuated by the pan-caspase inhibitor Z-VAD-FMK (Fig. 6C). TOP2A depletion using tetracycline almost halved caspase-3/7 activation by 1 $\mu\text{mol/L}$ doxorubicin (Fig. 6C, *top*) and abolished that evoked by dexrazoxane (Fig. 6C, *bottom*). Furthermore, doxorubicin (Fig. 6D), but not dexrazoxane (data not shown), cleaved the upstream activator of caspase-3/7, caspase-8. This effect was abolished following tetracycline pretreatment (Fig. 6D), indicating that caspase-8 acts downstream of TOP2A in response to doxorubicin.

These results clearly showed commonalities but also differences in cell-killing mechanisms by doxorubicin and

dexrazoxane. Common elements included TOP2A targeting resulting in DSB formation, involvement of mitochondrial p53, and activation of caspase-3/7. Doxorubicin-specific elements comprised GSH depletion and caspase-8 activation. The dexrazoxane-specific ones included the TOP2A depletion and the caspase-3/7-independent fraction of apoptosis in TOP2A-depleted cells (compare *bottom* of Fig. 6C with Fig. 2D). We therefore investigated the effects of both drugs, applied in various combinations of 100 $\mu\text{mol/L}$ dexrazoxane, 0.1 or 1 $\mu\text{mol/L}$ doxorubicin, and four incubation time schedules. Thus, in comparison with the 24 h incubation with doxorubicin (or control vehicle), dexrazoxane was applied during the preceding 0.5 h followed by washout (5 \times 5 min with PBS), simultaneously with doxorubicin (24 h), during the last 6 h of doxorubicin incubation (6 h), or throughout the entire experiment (24.5 h). As shown in Fig. 3A, addition of dexrazoxane clearly decreased DSB induced by 0.1 $\mu\text{mol/L}$ doxorubicin (dexrazoxane for 24.5, 24, and 6 h) and 1 $\mu\text{mol/L}$ doxorubicin (dexrazoxane for 24.5 h). This was accompanied, and most likely caused, by the already mentioned TOP2A depletion by dexrazoxane, which was more pronounced at 0.1 $\mu\text{mol/L}$ doxorubicin than that at 1.0 $\mu\text{mol/L}$ doxorubicin (Fig. 3A). Despite these effects on TOP2A level and DSB production,

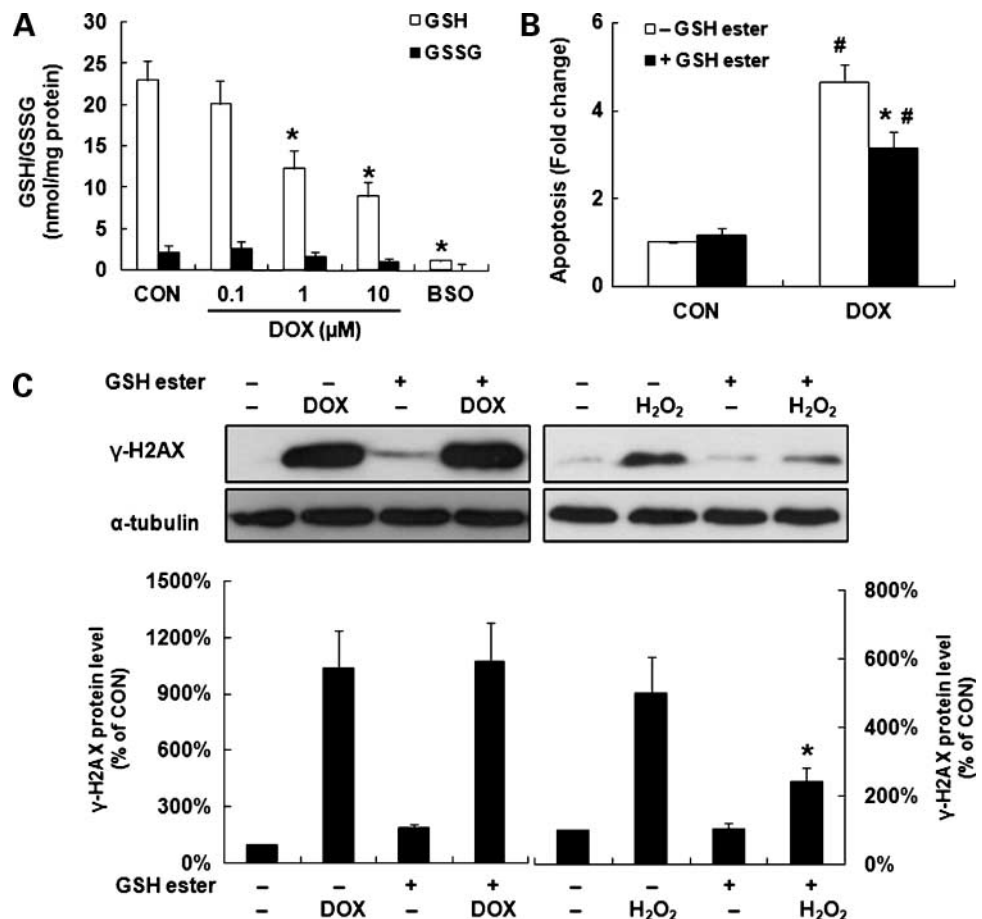


Figure 5. Role of intracellular glutathione in the doxorubicin response of HTETOP cells. **A**, GSH and GSSG content in cells following 24 h treatment with the indicated concentrations of doxorubicin or with buthionine sulfoximine (2 mmol/L). *, $P < 0.01$, compared with untreated cells. **B**, effect of coincubation with 10 mmol/L GSH ester on the apoptosis in response to 1 $\mu\text{mol/L}$ doxorubicin (24 h) assessed by Annexin V-FITC staining and FACS. #, $P < 0.05$, compared with doxorubicin-untreated cells; *, $P < 0.05$, compared with cells treated with doxorubicin but without GSH ethyl ester. **C**, effect of 10 mmol/L GSH ethyl ester on DSB formation assessed by Western blot as γ -H2AX foci in response to 100 $\mu\text{mol/L}$ H₂O₂ (2 h) or 1 $\mu\text{mol/L}$ doxorubicin (24 h) treatment. *, $P < 0.05$, compared with cells treated with H₂O₂ but without GSH ethyl ester.

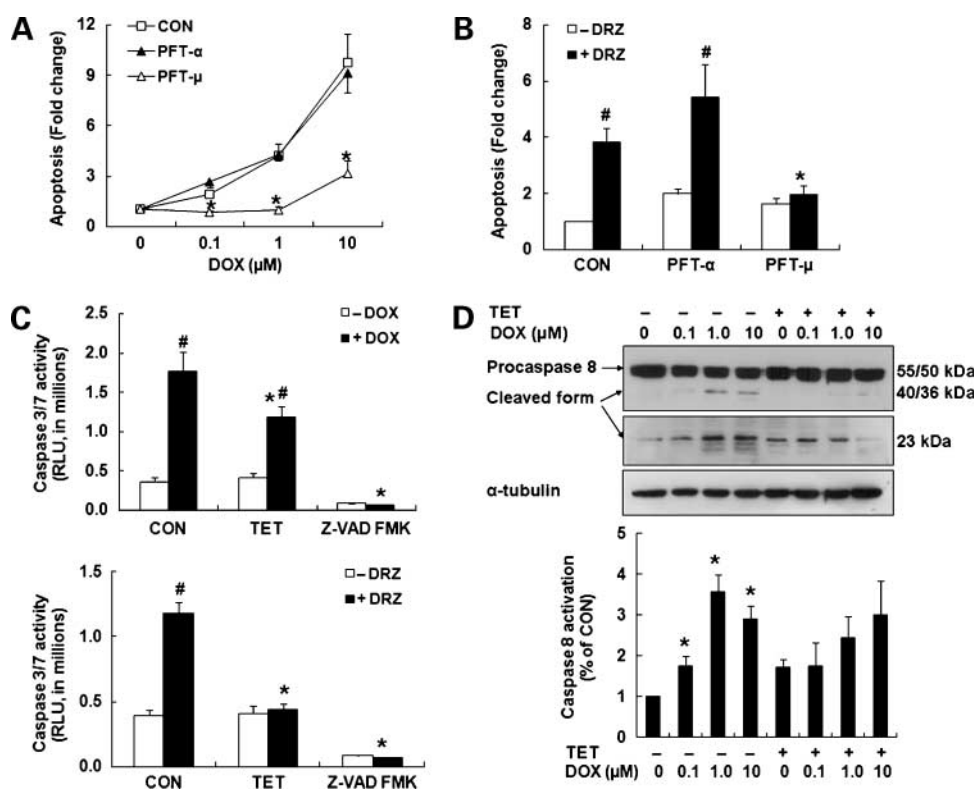


Figure 6. p53 and caspase activation in HTETOP cells treated with doxorubicin or dexrazoxane. **A**, apoptosis detected with Annexin V-FITC staining and FACS analysis in cells treated with doxorubicin for 24 h at the indicated concentrations with or without p53 inhibitor PFT- α (30 μ mol/L) or PFT- μ (30 μ mol/L). *, $P < 0.05$, compared with the same doxorubicin concentration but without p53 inhibitor. **B**, apoptosis detected by Annexin V-FITC staining and FACS analysis in cells exposed to 100 μ mol/L dexrazoxane for 24 h with or without p53 inhibitor PFT- μ (30 μ mol/L) or PFT- α (30 μ mol/L). #, $P < 0.05$, compared with dexrazoxane-untreated cells in the same group; *, $P < 0.05$, compared with dexrazoxane-treated cells. **C**, *top*, caspase-3/7 activity in response to 1 μ mol/L doxorubicin (24 h) in tetracycline-pretreated (1 μ g/mL, 24 h) or untreated cells and cells simultaneously treated with the pan-caspase inhibitor Z-VAD-FMK (20 μ mol/L). #, $P < 0.05$, compared with doxorubicin-untreated cells in the same group; *, $P < 0.05$, compared with untreated cells treated with doxorubicin. *Bottom*, dexrazoxane-induced (100 μ mol/L, 24 h) caspase-3/7 activation with or without prior TOP2A depletion with tetracycline (1 μ g/mL, 24 h) or cells simultaneously treated with Z-VAD-FMK (20 μ mol/L). #, $P < 0.05$, compared with dexrazoxane-untreated cells; *, $P < 0.05$, compared with dexrazoxane-treated cells. **D**, caspase-8 activation detected by Western blot in response to the indicated doxorubicin concentrations (24 h) with or without tetracycline pretreatment (1 μ g/mL, 24 h). Arrows, pro-caspase-8 and the cleaved forms. *, $P < 0.05$, compared with cells without any treatment.

dexrazoxane did not reduce apoptosis at any combination of doxorubicin concentration or incubation schedule (Fig. 3B). Quite the contrary, the extent of apoptosis in cells cotreated with 0.1 μ mol/L doxorubicin plus dexrazoxane was actually greater than in cells treated with 0.1 μ mol/L doxorubicin alone (Fig. 3B, *middle*). Similar results were also observed in two other tumor cell lines, A549 and DLD1 (data not shown). Finally, TOP2A depletion by tetracycline pretreatment of HTETOP cells reduced by 30% ($P < 0.02$) the apoptotic response to the combination of 1 μ mol/L doxorubicin and 100 μ mol/L dexrazoxane over 24 h (data not shown). This indicated that apoptosis was mediated by both TOP2A-dependent and TOP2A-independent mechanisms as was observed when each drug was applied alone (Fig. 2C and D).

Discussion

The replacement in HTETOP cells of the endogenous TOP2A gene by a tetracycline-responsive transgene allows for bypassing the cellular lethality of TOP2A deletion. Phe-

notypic differences between tetracycline-treated and untreated cells reflect chiefly the effects of TOP2A, because its depletion occurs in the absence of any changes in the expression of other genes (Fig. 2A) and in cell cycle distribution within the first 48 h (13). This allowed, for the first time, to clearly differentiate between TOP2A-dependent and TOP2A-independent effects of doxorubicin. Using this tool, we also assessed the cancer cell-killing mechanisms of dexrazoxane, which is administered to cancer patients to prevent the cardiotoxic side effects of doxorubicin and other anthracyclines. The results suggest an explanation for the absence of adverse dexrazoxane effects on cancer treatments with doxorubicin despite these drugs sharing TOP2A as their major molecular target. The explanation lies in the TOP2A-independent component of the apoptosis triggered by each drug, which compensates for the dexrazoxane-induced TOP2A depletion and associated reduction in doxorubicin-induced DSB. To arrive at this conclusion, we first had to characterize the importance of TOP2A in the apoptotic effects of each drug.

Doxorubicin-Induced Apoptosis Involves TOP2A Inhibition and GSH Depletion

DSB formation and apoptosis are mediated exclusively by TOP2A only at low doxorubicin concentrations (0.1 $\mu\text{mol/L}$). At higher doxorubicin concentrations, roughly half of the doxorubicin-induced apoptosis is TOP2A independent (Fig. 2C). This finding is important in the light of current efforts to develop TOP2A expression level as a predictor of doxorubicin response in breast cancer (9). Such a predictive value of TOP2A is at present controversial, because some studies found only weak correlations between tumor response to doxorubicin and TOP2A expression levels (28). Our data indicate that this may be caused, at least in part, by the confounding contribution of TOP2A-independent apoptotic pathways.

TOP2A-independent apoptosis pathways may nevertheless be useful for optimizing doxorubicin treatments and so deserve further investigation. A major portion of doxorubicin-induced apoptosis in HTETOP cells appears to be triggered by a pronounced depletion of total cellular glutathione. Glutathione depletion by doxorubicin has been reported in a recent study (29) and intracellular glutathione levels are remarkably specific predictors of doxorubicin-induced cell growth inhibition (30). The glutathione depletion could be caused by outward cotransport of doxorubicin and glutathione by the multidrug resistance protein 1 (31) or by inhibition of glutathione synthesis (23). Irrespective of the exact mechanism, the depletion contributes to, rather than results from, doxorubicin-induced apoptosis in HTE-TOP cells, because cell death is reduced by glutathione supplementation (Fig. 5B). The TOP2A and glutathione depletion most likely represent nonoverlapping apoptotic pathways. Indeed, although both TOP2A depletion and GSH supplementation diminish doxorubicin-induced apoptosis (Figs. 2C and 5B), only the former reduces the associated DSB (Figs. 1A and 5C). We detected no evidence for oxidative stress due to "redox cycling" of doxorubicin as judged from the remarkably constant proportion of GSSG in the total intracellular glutathione pool following doxorubicin treatment (Fig. 5A). This is consistent with the growing evidence that oxidative stress due to doxorubicin "redox cycling" plays no role in cancer cell killing at clinically relevant concentrations of the drug (10).

A portion of DSB induced by $\geq 1 \mu\text{mol/L}$ doxorubicin was refractory to TOP2A depletion (Fig. 1A) and/or glutathione supplementation (Fig. 5C), indicating the existence of further mechanisms of DSB generation. Likely candidates include the multifarious direct interactions between doxorubicin and DNA (10) or the doxorubicin poisoning of TOP2B, which is expressed in HTETOP cells, albeit at a much lower level than TOP2A (13). TOP2B could also mediate a portion of TOP2A-independent apoptosis in response to doxorubicin. Oxidative stress was probably not involved in DSB formation, because, as already stated, glutathione ethyl ester did not reduce doxorubicin-induced DSB accumulation.

Dexrazoxane Decreases TOP2A Transcript Level

The dexrazoxane-induced formation of DSB was fully tetracycline sensitive (Fig. 1B), suggesting that the DSB are ex-

clusively TOP2A derived. This supports previous reports of dexrazoxane and other bisdioxopiperazines being TOP2A "poisons" in addition to the inhibition of the catalytic activity of the enzyme (12, 32). The molecular mechanism of TOP2A "poisoning" could involve TOP2A targeting beyond the ATPase-bearing NH_2 -terminal domain as shown for a *Drosophila* TOP2 and the related bisdioxopiperazine ICRF-159 (33). Dexrazoxane-induced apoptosis in HTETOP cells is in agreement with several previous studies of cancer-derived cells (34-36), but its mechanism remains poorly understood. Our data clearly show the involvement of TOP2A, because apoptosis was partly reduced by tetracycline (Fig. 2D).

Like cardiomyocytes (20), HTETOP cells respond to dexrazoxane by degradation of the TOP2B protein (Fig. 4D), indicating that this effect is not heart exclusive. At the mRNA level, dexrazoxane affected the expression of only two genes, activating transcription factor 3 and TOP2A. The remarkable specificity of dexrazoxane-induced gene expression changes contrasts with effects of doxorubicin and other oncologic drugs, which usually affect hundreds of genes (37). This is important in the context of further development of dexrazoxane as simultaneously anticancer and organ-protective agent. Activating transcription factor 3 is proapoptotic in several cancer cell lines (38, 39), but it protects cardiomyocytes against doxorubicin-induced cell death (40). Activating transcription factor 3 may be a specific and central determinant of the disparate and cell type-specific outcomes of dexrazoxane exposure such as cell death and cell protection.

The reduced expression of TOP2A mRNA in response to dexrazoxane was reflected by reduced levels of TOP2A protein. Dexrazoxane-induced depletion of TOP2A transcripts was observed in both HTETOP and parental HT1080 cells, which transcribe TOP2A mRNA from totally different promoters. It seems unlikely, therefore, that this new and unexpected effect of dexrazoxane involves reduced transcriptional initiation, but transcript degradation, repression of transcriptional elongation, or termination may be responsible. TOP2A depletion following dexrazoxane treatment in HTETOP cells contrasts, at least at a first glance, with the absence of such an effect in cardiomyocytes (20). However, the effects of dexrazoxane on TOP2A in cardiomyocytes were investigated over short periods of time (≤ 60 min), whereas, in HTETOP, the decrease in TOP2A cells was only detectable 12 h after dexrazoxane addition (Supplementary Fig. B).³ It should also be emphasized that we detected the dexrazoxane-associated TOP2A decrease in HTETOP cells at both protein and mRNA levels using three different methods (Western blot, TaqMan, and RNA chips). The exact mechanisms of dexrazoxane-induced TOP2A depletion require more detailed studies, which are currently ongoing. Because dexrazoxane binds and inhibits the TOP2A protein, the simplest hypothesis is that the enzyme regulates its own transcript level.

No Adverse Effect of Dexrazoxane on Doxorubicin-Induced Apoptosis

TOP2A depletion by dexrazoxane could reasonably be expected to reduce the TOP2A-dependent portion of apoptosis

by doxorubicin. This is indeed the case in respect of doxorubicin-induced DSB, which are clearly reduced, along with the TOP2A level, in cells coexposed to dexrazoxane (Fig. 3A). Dexrazoxane-dependent reductions in DSB induction and TOP2A levels are especially pronounced in HTETOP cells exposed to 0.1 $\mu\text{mol/L}$ doxorubicin. Considering that dexrazoxane depletes TOP2A (Fig. 4A) and that apoptosis induced by 0.1 $\mu\text{mol/L}$ doxorubicin is completely dependent on TOP2A (Fig. 2C), the majority of apoptosis in response to 0.1 $\mu\text{mol/L}$ doxorubicin combined with dexrazoxane must be induced by dexrazoxane. In support of this conclusion, dexrazoxane combined with 0.1 $\mu\text{mol/L}$ doxorubicin induces levels of apoptosis similar to, or greater than, those induced by 0.1 $\mu\text{mol/L}$ doxorubicin alone (Fig. 3B) despite the much lower accumulation of DSB (Fig. 3A). Thus, dexrazoxane-induced apoptosis fully compensates for the reduction of 0.1 $\mu\text{mol/L}$ doxorubicin-induced apoptosis due to dexrazoxane-induced TOP2A depletion. When applied with 1 $\mu\text{mol/L}$ doxorubicin, dexrazoxane still reduces doxorubicin-induced DSB, especially significant for coincubation periods of 24.5 h (Fig. 3A). The depletion of TOP2A by dexrazoxane is, however, less pronounced under these conditions than on coincubation with 0.1 $\mu\text{mol/L}$ doxorubicin. This can be explained by the accumulation of doxorubicin-“poisoned” TOP2A, which is higher at 1 $\mu\text{mol/L}$ than 0.1 $\mu\text{mol/L}$ doxorubicin, and may partly offset the TOP2A-depleting effect of dexrazoxane. Thus, as for 0.1 $\mu\text{mol/L}$ doxorubicin, apoptosis induced by 1 $\mu\text{mol/L}$ doxorubicin is not diminished by dexrazoxane in any of the tested incubation schedules (Fig. 3B).

This apparent contradiction between dexrazoxane-dependent reductions in TOP2A and doxorubicin-induced DSB on one hand and the absence of any dexrazoxane-dependent reductions in doxorubicin-induced apoptosis on the other hand can be explained by the TOP2A-independent apoptosis effects of each drug. Those of doxorubicin clearly involve glutathione depletion as well as DSB formation via an unknown mechanism. TOP2B is unlikely to contribute, because it is depleted by dexrazoxane (Fig. 4D), in agreement with previous studies (20). The TOP2A-independent component of dexrazoxane-induced apoptosis is at present more enigmatic, but it is dependent on the mitochondrial p53 and may involve caspase-independent apoptotic pathways. Indeed, unlike the caspase-3/7 activity itself, the TOP2A-independent fraction of apoptosis evoked by dexrazoxane was insensitive to the pan-caspase inhibitor Z-VAD-FMK. The involvement of mitochondrial p53 is in agreement with previous reports of dexrazoxane-induced apoptosis being modulated by Bcl-xL (36).

Taken together, doxorubicin and dexrazoxane may interact in cancer cells such as HTETOP via several different mechanisms. The overlapping component comprises inhibition of TOP2A by both drugs, in each case resulting in DSB formation and apoptosis. Dexrazoxane interacts with the doxorubicin response via degradation of the doxorubicin target TOP2A, which explains the reduction in total DSB accumulation observed on combination of these drugs. Despite this interaction, dexrazoxane does not compromise the apopto-

tic activity of doxorubicin. This is caused by the compensating contribution of TOP2A-independent apoptosis evoked by both drugs. These results suggest a mechanistic explanation for the absence of adverse effects of dexrazoxane on anthracycline treatments, recently confirmed in a meta-analysis conducted by the Cochrane Collaboration (3). Under circumstances exemplified by low doxorubicin availability, dexrazoxane seems actually to enhance the net extent of HTETOP cell killing. This is in agreement with early observations in several animal cancer models (7) as well as with dexrazoxane having doubled the mean survival time of breast cancer patients who responded to doxorubicin (41).

Disclosure of Potential Conflicts of Interest

L. Wojnowski: Dexrazoxane Advisory Board of Novartis. No other potential conflicts of interest were disclosed.

Acknowledgments

We thank Drs. Lars-Oliver Klotz, Markus Christmann, Gerhard Fritz, and Bernd Kaina for discussions and suggestions during the course of the work and Drs. Heidi Hahn and Simone Fulda for comments on the article.

References

1. Minotti G, Menna P, Salvatorelli E, Cairo G, Gianni L. Anthracyclines: molecular advances and pharmacologic developments in antitumor activity and cardiotoxicity. *Pharmacol Rev* 2004;56:185–229.
2. van Dalen EC, van der Pal HJ, Kok WE, Caron HN, Kremer LC. Clinical heart failure in a cohort of children treated with anthracyclines: a long-term follow-up study. *Eur J Cancer* 2006;42:3191–8.
3. van Dalen EC, Caron HN, Dickinson HO, Kremer LC. Cardioprotective interventions for cancer patients receiving anthracyclines. *Cochrane Database Syst Rev* 2008;2:DOI:10.1002/14651858.CD003917.pub3.
4. Hasinoff BB, Herman EH. Dexrazoxane: how it works in cardiac and tumor cells. Is it a prodrug or is it a drug? *Cardiovasc Toxicol* 2007;7:140–4.
5. Moghrabi A, Levy DE, Asselin B, et al. Results of the Dana-Farber Cancer Institute ALL Consortium Protocol 95-01 for children with acute lymphoblastic leukemia. *Blood* 2007;109:896–904.
6. Hasinoff BB, Yalowich JC, Ling Y, Buss JL. The effect of dexrazoxane (ICRF-187) on doxorubicin- and daunorubicin-mediated growth inhibition of Chinese hamster ovary cells. *Anticancer Drugs* 1996;7:558–67.
7. Hasinoff BB, Hellmann K, Herman EH, Ferrans VJ. Chemical, biological and clinical aspects of dexrazoxane and other bisdioxopiperazines. *Curr Med Chem* 1998;5:1–28.
8. Larsen AK, Escargueil AE, Skladanowski A. Catalytic topoisomerase II inhibitors in cancer therapy. *Pharmacol Ther* 2003;99:167–81.
9. Faratian D, Bartlett J. Predictive markers in breast cancer—the future. *Histopathology* 2008;52:91–8.
10. Gewirtz DA. A critical evaluation of the mechanisms of action proposed for the antitumor effects of the anthracycline antibiotics Adriamycin and daunorubicin. *Biochem Pharmacol* 1999;57:727–41.
11. Jensen LH, Nitiss KC, Rose A, et al. A novel mechanism of cell killing by anti-topoisomerase II bisdioxopiperazines. *J Biol Chem* 2000;275:2137–46.
12. Huang KC, Gao H, Yamasaki EF, et al. Topoisomerase II poisoning by ICRF-193. *J Biol Chem* 2001;276:44488–94.
13. Carpenter AJ, Porter AC. Construction, characterization, and complementation of a conditional-lethal DNA topoisomerase II α mutant human cell line. *Mol Biol Cell* 2004;15:5700–11.
14. Akimitsu N, Adachi N, Hirai H, et al. Enforced cytokinesis without complete nuclear division in embryonic cells depleting the activity of DNA topoisomerase II α . *Genes Cells* 2003;8:393–402.
15. Vandeputte C, Guizon I, Genestie-Denis I, Vannier B, Lorenzon G. A

- microtiter plate assay for total glutathione and glutathione disulfide contents in cultured/isolated cells: performance study of a new miniaturized protocol. *Cell Biol Toxicol* 1994;10:415–21.
16. Deng S, Kulle B, Hosseini M, et al. Dystrophin-deficiency increases the susceptibility to doxorubicin-induced cardiotoxicity. *Eur J Heart Fail* 2007;9:986–94.
 17. Irizarry RA, Hobbs B, Collin F, et al. Exploration, normalization, and summaries of high density oligonucleotide array probe level data. *Biostatistics* 2003;4:249–64.
 18. Rogakou EP, Pilch DR, Orr AH, Ivanova VS, Bonner WM. DNA double-stranded breaks induce histone H2AX phosphorylation on serine 139. *J Biol Chem* 1998;273:5858–68.
 19. Kotamraju S, Konorev EA, Joseph J, Kalyanaraman B. Doxorubicin-induced apoptosis in endothelial cells and cardiomyocytes is ameliorated by nitron spin traps and ebselen. Role of reactive oxygen and nitrogen species. *J Biol Chem* 2000;275:33585–92.
 20. Lyu YL, Kerrigan JE, Lin CP, et al. Topoisomerase II β mediated DNA double-strand breaks: implications in doxorubicin cardiotoxicity and prevention by dexrazoxane. *Cancer Res* 2007;67:8839–46.
 21. Zhang A, Lyu YL, Lin CP, et al. A protease pathway for the repair of topoisomerase II-DNA covalent complexes. *J Biol Chem* 2006;281:35997–6003.
 22. Classen S, Olland S, Berger JM. Structure of the topoisomerase II ATPase region and its mechanism of inhibition by the chemotherapeutic agent ICRF-187. *Proc Natl Acad Sci U S A* 2003;100:10629–34.
 23. Griffith OW, Meister A. Potent and specific inhibition of glutathione synthesis by buthionine sulfoximine (*S-N*-butyl homocysteine sulfoximine). *J Biol Chem* 1979;254:7558–60.
 24. Hochhauser D, Valkov NI, Gump JL, et al. Effects of wild-type p53 expression on the quantity and activity of topoisomerase II α and β in various human cancer cell lines. *J Cell Biochem* 1999;75:245–57.
 25. Ao Y, Rohde LH, Naumovski L. p53-interacting protein 53BP2 inhibits clonogenic survival and sensitizes cells to doxorubicin but not paclitaxel-induced apoptosis. *Oncogene* 2001;20:2720–5.
 26. Strom E, Sathé S, Komarov PG, et al. Small-molecule inhibitor of p53 binding to mitochondria protects mice from gamma radiation. *Nat Chem Biol* 2006;2:474–9.
 27. Komarov PG, Komarova EA, Kondratov RV, et al. A chemical inhibitor of p53 that protects mice from the side effects of cancer therapy. *Science* 1999;285:1733–7.
 28. Jarvinen TA, Holli K, Kuukasjarvi T, Isola JJ. Predictive value of topoisomerase II α and other prognostic factors for epirubicin chemotherapy in advanced breast cancer. *Br J Cancer* 1998;77:2267–73.
 29. Sharma A, Patrick B, Li J, et al. Glutathione *S*-transferases as antioxidant enzymes: small cell lung cancer (H69) cells transfected with hGSTA1 resist doxorubicin-induced apoptosis. *Arch Biochem Biophys* 2006;452:165–73.
 30. Bracht K, Grunert R, Bednarski PJ. Correlations between the activities of 19 anti-tumor agents and the intracellular glutathione concentrations in a panel of 14 human cancer cell lines: comparisons with the National Cancer Institute data. *Anticancer Drugs* 2006;17:41–51.
 31. Renes J, de Vries EG, Nienhuis EF, Jansen PL, Muller M. ATP- and glutathione-dependent transport of chemotherapeutic drugs by the multidrug resistance protein MRP1. *Br J Pharmacol* 1999;126:681–8.
 32. Wang L, Eastmond DA. Catalytic inhibitors of topoisomerase II are DNA-damaging agents: induction of chromosomal damage by merbarone and ICRF-187. *Environ Mol Mutagen* 2002;39:348–56.
 33. Chang S, Hu T, Hsieh TS. Analysis of a core domain in *Drosophila* DNA topoisomerase II. Targeting of an antitumor agent ICRF-159. *J Biol Chem* 1998;273:19822–8.
 34. Khelifa T, Beck WT. Induction of apoptosis by dexrazoxane (ICRF-187) through caspases in the absence of c-jun expression and c-Jun NH₂-terminal kinase 1 (JNK1) activation in VM-26-resistant CEM cells. *Biochem Pharmacol* 1999;58:1247–57.
 35. Morgan SE, Cadena RS, Raimondi SC, Beck WT. Selection of human leukemic CEM cells for resistance to the DNA topoisomerase II catalytic inhibitor ICRF-187 results in increased levels of topoisomerase II α and altered G(2)/M checkpoint and apoptotic responses. *Mol Pharmacol* 2000;57:296–307.
 36. Hasinoff BB, Abram ME, Barnabe N, Khelifa T, Allan WP, Yalowich JC. The catalytic DNA topoisomerase II inhibitor dexrazoxane (ICRF-187) induces differentiation and apoptosis in human leukemia K562 cells. *Mol Pharmacol* 2001;59:453–61.
 37. Zembutsu H, Ohnishi Y, Tsunoda T, et al. Genome-wide cDNA microarray screening to correlate gene expression profiles with sensitivity of 85 human cancer xenografts to anticancer drugs. *Cancer Res* 2002;62:518–27.
 38. Syed V, Mukherjee K, Lyons-Weiler J, et al. Identification of ATF-3, caveolin-1, DLC-1, and NM23-2 as putative antitumorigenic, progesterone-regulated genes for ovarian cancer cells by gene profiling. *Oncogene* 2005;24:1774–87.
 39. Fan F, Jin S, Amundson SA, et al. ATF3 induction following DNA damage is regulated by distinct signaling pathways and over-expression of ATF3 protein suppresses cells growth. *Oncogene* 2002;21:7488–96.
 40. Nobori K, Ito H, Tamamori-Adachi M, et al. ATF3 inhibits doxorubicin-induced apoptosis in cardiac myocytes: a novel cardioprotective role of ATF3. *J Mol Cell Cardiol* 2002;34:1387–97.
 41. Swain SM, Whaley FS, Gerber MC, Ewer MS, Bianchine JR, Gams RA. Delayed administration of dexrazoxane provides cardioprotection for patients with advanced breast cancer treated with doxorubicin-containing therapy. *J Clin Oncol* 1997;15:1333–40.